Journal of Engineering and Applied Technology
Vol. 5, No. 1, March 2024, pp. 52-64

Online ISSN 2716-2265
Printed ISSN 2716-2257

Soil liquefaction measurement and adjustment system on shaking table for seismic simulation

Mahmud Abdul Karim[1], Dea Aulia Sakinah[1], Dimas Nugroho Nuradryanto[1], Sulis Setiowati[1,*], Rika Novita Wardhani[1], A'isyah Salimah[2], Yelvi[2]

[1] Departement of Electrical Engineering, Jakarta State Polytechnic, Indonesia
[2] Departement of Civil Engineering, Jakarta State Polytechnic, Indonesia
E-mail: sulis.setiowati@elektro.pnj.ac.id *
* Corresponding Author

ABSTRACT

The liquefaction simulator tool uses a one-axis shaking table model to determine soil features and behaviour that indicate liquefaction. This helps in implementing measures to mitigate its effects. The research system incorporates a frequency regulation system to control the speed of the 3-phase motor and a measurement system that monitors various variables associated with liquefaction. The variables include displacement, rocking table motion, acceleration, vibration frequency, and pore water pressure. This study used LabVIEW for frequency adjustment, data acquisition, processing, and presentation. LabVIEW improved the observations' accuracy using the linear regression method and descriptive statistical analysis at the data processing stage. The error value for the frequency adjustment without load was 1.65%, which increased to 8.75% when a load was applied. This study achieved a displacement measurement accuracy of 99.03% and an average pore water pressure measurement accuracy of 95.69%. The measurement accuracy of the accelerometer and accelerometer vibration frequency reached 66.98%.

ARTICLE INFO

Article history
Received:
27 August 2023
Revised:
30 March 2024
Accepted:
31 March 2024

Keywords
acceleration
displacement
frequency
pore water pressure
shaking table
soil liquefaction

1. Introduction

Shaking tables are capable of replicating field conditions during earthquake shaking, thus facilitating in-depth studies on the potential occurrence of liquefaction events [1], [2]. Shaking tables play an important role in investigating the liquefaction phenomenon, which can then be applied in the field to mitigate the impact of this phenomenon. The responses investigated in this study include excess pore pressure, acceleration, and earthquake frequency in the soil [3], [4], [5]. The importance of observing pore water pressure, acceleration, and frequency responses during earthquakes underscores the need for effective measurement systems that are responsive and highly accurate in detecting any changes that arise within the facility [6]. Tests on shaking tables usually follow conventional methods, such as adjusting a variable transformer to regulate motor speed, which offers a limited range of input settings for motor speed adjustment. In addition, measurements often face the challenge of human error [7]. To minimize such errors, efficient, responsive, and highly accurate measurement and control systems should be used, by integrating the technology into digital systems. Data obtained from control and measurement systems can be displayed on a Human Machine Interface (HMI), thereby increasing the convenience of data analysis and observation.

The integration of control and measurement systems anticipated with LabVIEW is expected to solve problems related to setting frequencies on vibration tables and measuring responses such as pore water pressure, acceleration, and frequency during soil testing using a soil liquefaction simulator. This

integration is ready to improve system performance [9], [10], [11]. The shaking table uses LabVIEW technology for frequency configuration, data acquisition, processing, and presentation. This technology supports observation through the linear regression method and descriptive statistical analysis, thereby facilitating the processing of measurement data [12] - [15].

2. Method

This soil liquefaction simulator, based on LabVIEW, employs a research methodology that includes several stages from tool design to tool implementation. The study involves the hardware and software design of a soil liquefaction simulator utilizing LabVIEW 2015.

2.1. Hardware System Design

The study involving a shaking table employs a rigid box model that moves horizontally along a single axis. The inner test box measures 400 x 400 x 600 mm, with a load capacity of ± 150 kg, as depicted in Fig. 1(a). The rigid box was made of transparent acrylic material, 10 mm in thickness, allowing for visual observation of soil behaviour during the test.

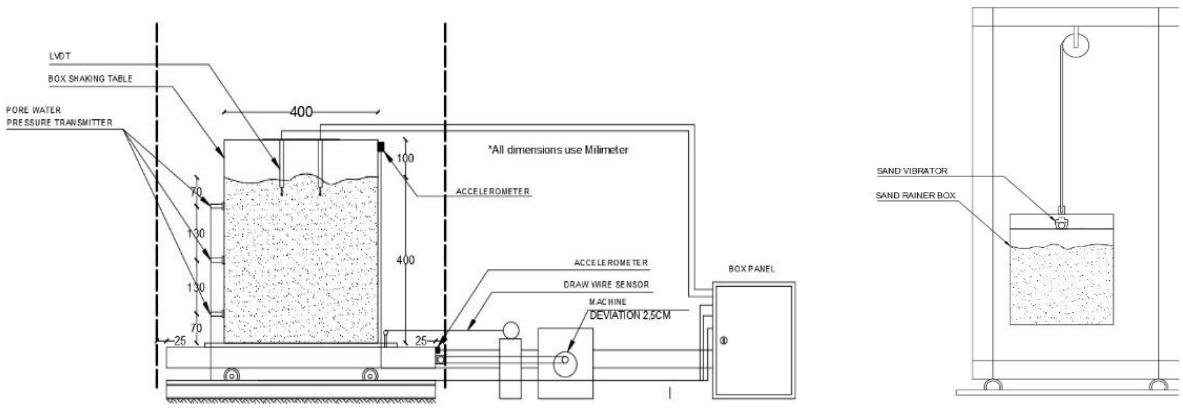

(a) (b)

Fig 1. (a) Design of shaking table (b) Design of sand rainer box

Additionally, as shown in Fig. 1(b), there is a sand rainer box equipped with a pulley, designed for releasing sand into the test box. The pulley system aids in controlling the height of the sand's descent, ensuring consistent density of the used sand material. Both the shaking table and the sand rainer box are strategically positioned to function as a soil liquefaction simulator, as illustrated in Fig. 2.

The soil liquefaction simulator's control and measurement system consists of three system elements, namely input, process and output systems, as shown in Fig. 3. According to the block diagram shown in Fig. 3, the input block contains the necessary components to execute the detection function as the system input.

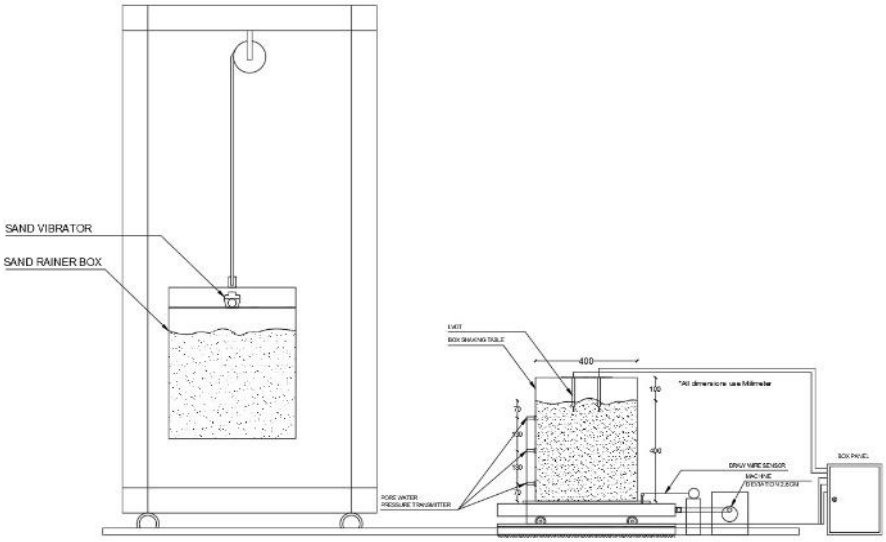

Fig 2. The placement of the shaking table and sand rainer box

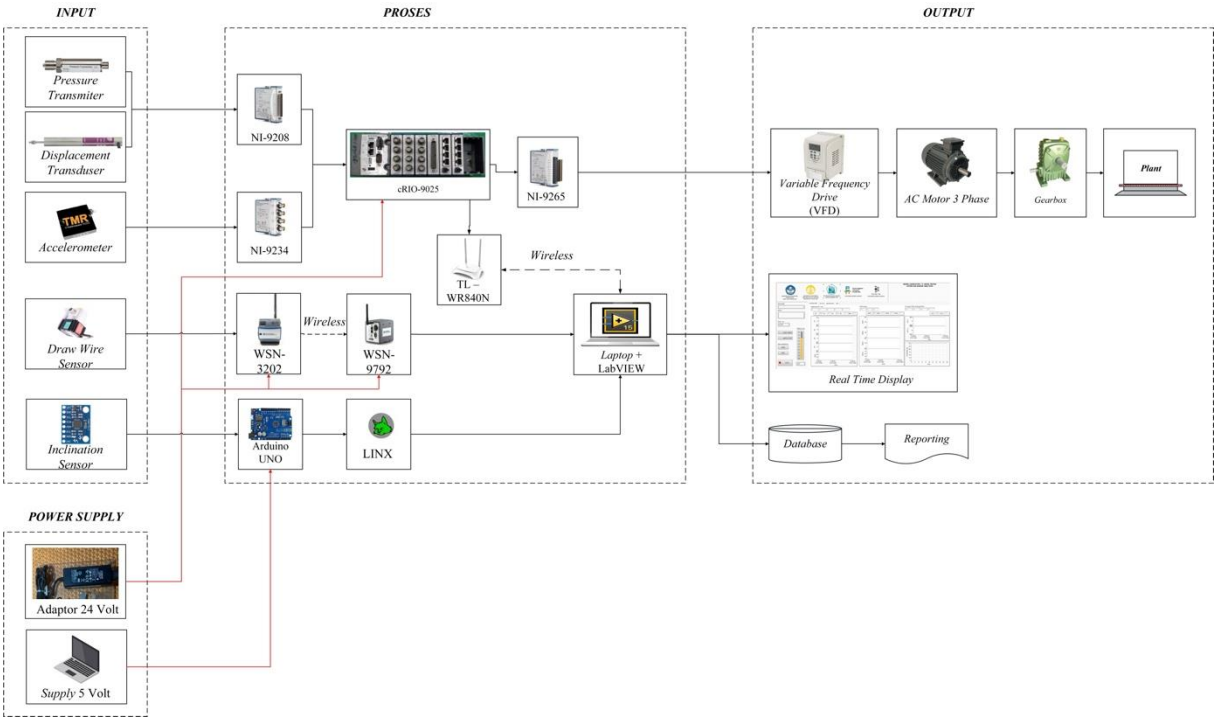

Fig 3. Block diagram of system

The input is processed in the process block. The input block consists of three pressure transmitters, one draw-wire sensor, and two accelerometers. The process block consists of a cRIO-9025 microcontroller for data processing, NI 9028 modules for pressure transmitter inputs, NI 9234 modules for accelerometer inputs, WSN 3202 and WSN 9792 modules for draw-wire sensor inputs, NI 9265 modules for current outputs connected to VFDs, and TL-WR840N for wireless communication. In the

output section, a Real-Time Display serves as the Human Machine Interface (HMI) for the system. In addition, VFDs, 3-phase motors and gearboxes are responsible for facilitating the movement of the plant.

2.2 Software System Design

The software system design employed for adjusting frequency, acquiring data, processing data, and displaying data in this study is LabVIEW 2015. A flow chart illustrating the system's overall functioning was created during the software design process, as shown in Fig. 4.

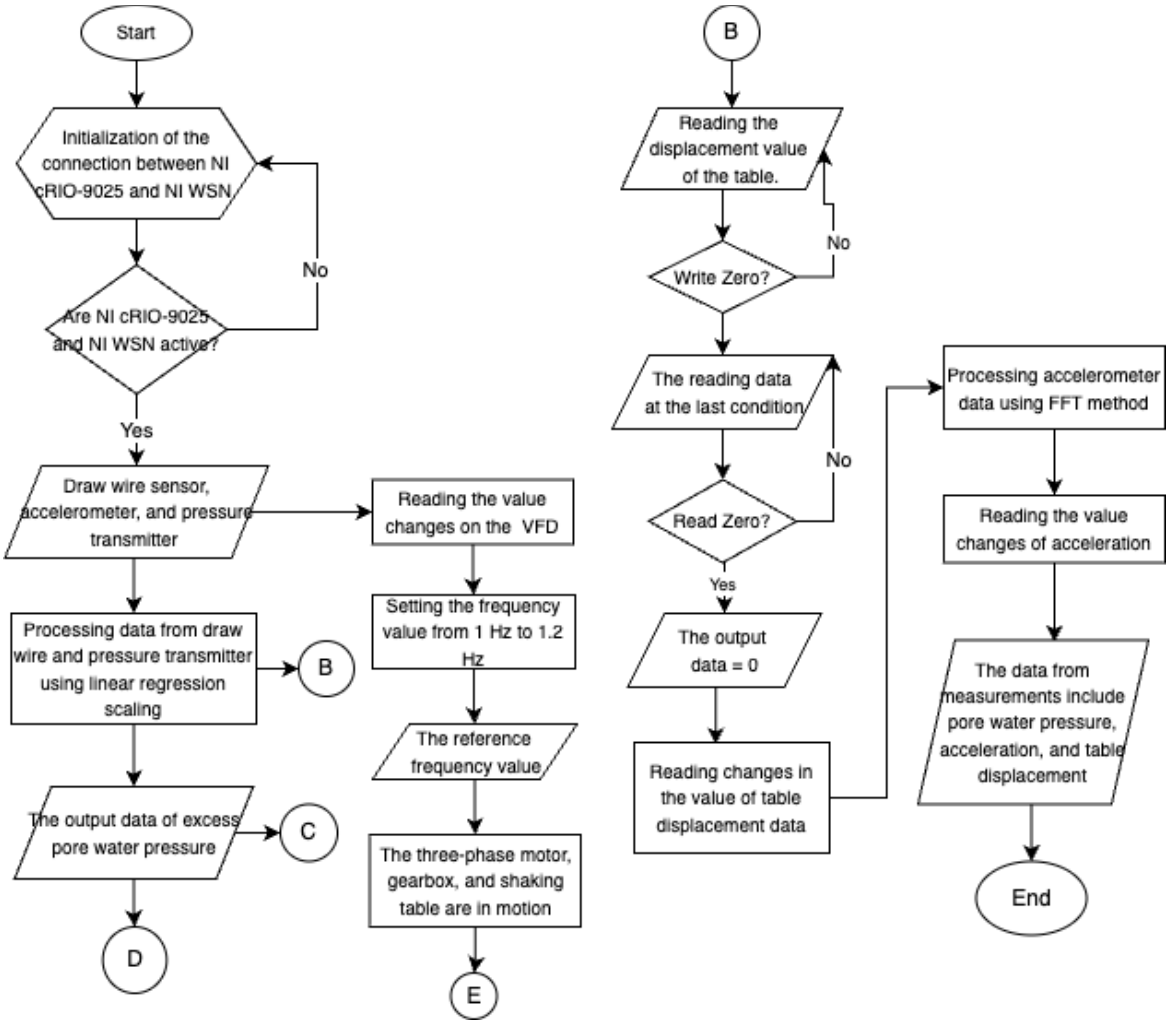

Fig 4. Flowchart of system arrangement and measurement system

Based on the flowchart illustrated in Fig. 4, it can be seen how the system works, starting with the initialization of the cRIO-9025 input, which then adjusts the frequency value required for the test. Furthermore, the system will receive input from a draw-wire sensor, accelerometer, and pressure transmitter to gather data for processing using the linear regression scaling method. This will generate the value of the pore water pressure in the soil and the displacement on the table. After obtaining the displacement value variable, proceed with collecting data in the array to determine whether to write zero. If the condition is met, the last condition will generate a value, while a read zero decision will produce a data value of zero. When the variable data changes, a measurement of table deviation will be produced. The accelerometer employs the Fast Fourier Transform (FFT) method to process the input

data and obtain acceleration and frequency values. The resulting data in the form of soil displacement, pore pressure, acceleration, and frequency will be displayed on the HMI to show the variable value data.

2.3 Implementation of System

In the implementation step, the realisation of the previously designed hardware and software design was carried out. This involved the realization of the hardware design, specifically the 1-axis shaking table and sand rainer box, as illustrated in Fig. 5.

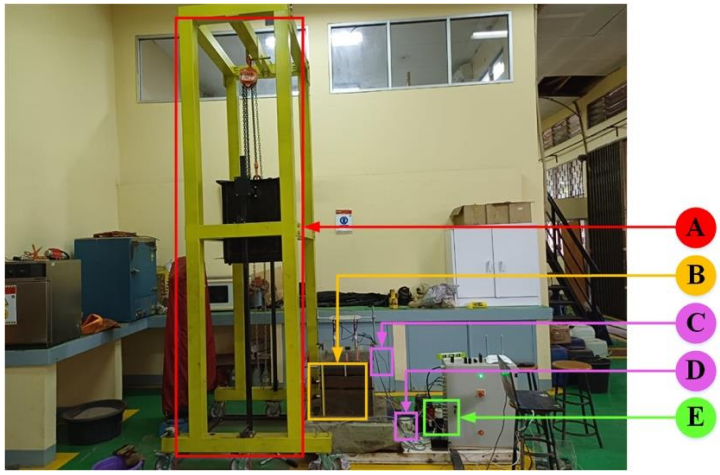

Fig 5. Integration of hardware system

Fig. 5 shows the entire hardware system, consisting of point A as a sand rainer box, point B as a 1-axis shaking table and pressure transmitter sensor placement, point C as the placement of accelerometer 1, point D as the placement of accelerometer 2, and point E is the placement of the draw-wire sensor.

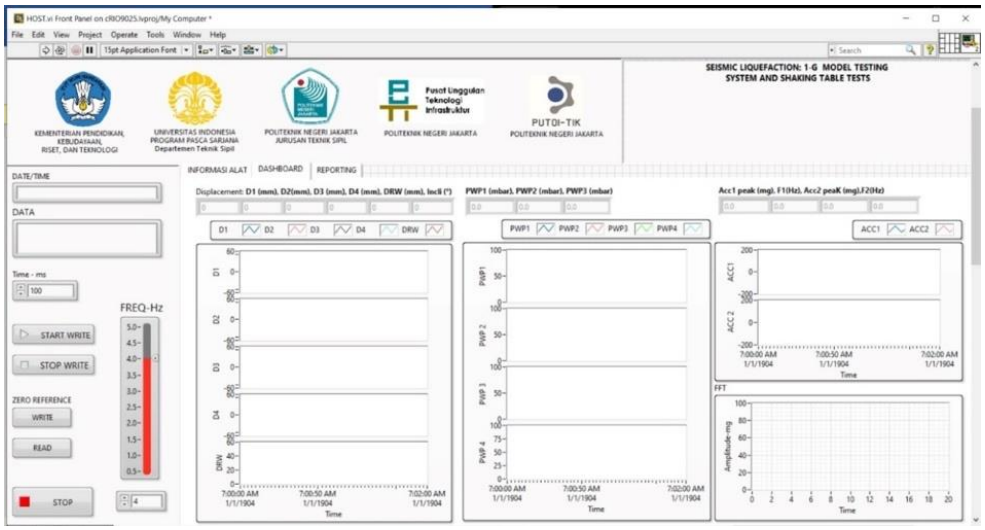

Fig 6. Front panel display on LabVIEW

Fig. 6 realizes the integration between the frequency adjustment system and the measurement of pore pressure in the soil, displacement and acceleration of the vibration frequency displayed on the LabVIEW front panel, which becomes the HMI display.

3. Results and Discussion

The results of the research are the response of the frequency adjustment system using a VFD and the measurement system, namely excess pore water pressure, displacement, acceleration, and vibration frequency.

3.1. Response of frequency measurement

In this study, the speed of a three-phase motor was adjusted using frequency regulation. The frequency can be altered from 0-5 Hz, but for the purposes of shaking conditions, the frequencies used are 1 Hz and 1.2 Hz. The frequency values are calculated by converting the earthquake intensity based on the BMKG SIG scale and the response data of the frequency adjustment with and without load by comparing the frequency value and the tachometer, as shown in Table 1.

Table 1. Comparison of VFD validation testing process results with and without with a tachometer

Sample number	Measurement results of excess pore water pressure without load (mbar)				
	Input frequency of LabVIEW (Hz)	Frequency of VFD (Hz)	Tachometer or speed of motor (rpm)	Frequency of motor (Hz)	Error (%)
1	1.0	10	573	9.5	1.65
2	1.2	12	709	11.81	
Sample number	**Measurement results of excess pore water pressure with load (mbar)**				
	Input frequency of LabVIEW (Hz)	**Frequency of VFD (Hz)**	**Tachometer or speed of motor (rpm)**	**Frequency of motor (Hz)**	**Error (%)**
1	1.0	10	535.7	8.93	8.71
2	1.2	12	676.4	11.27	

Based on Table 1, the data was analyzed and an error value of 1.65% was calculated for no load, while an error value of 8.71% was calculated for load. The error value allows for the determination of the acceptable frequency error limit for the motor by comparing it with the frequency-based tolerance provision of ±5% [16]. Therefore, the frequency received by the motor without a load can be categorized as being within the tolerance limit, as it is only reduced by approximately ± 2%.

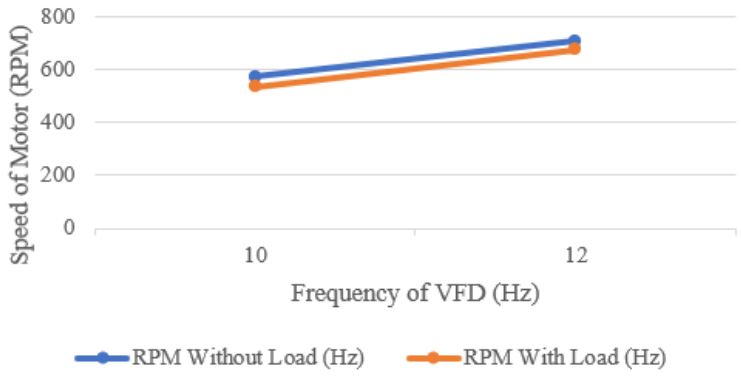

Fig 7. The relationship of motor speed to frequency with and without load

In addition, Fig. 7 illustrates that the relationship between motor speed and frequency is directly proportional, which means that the greater the frequency input, the faster the motor speed.

3.2 Response of excess pore water pressure measurement

Based on this research, the response data of excess pore water pressure measurement measured by the pressure transmitter for 60 seconds or when the shaking table condition is given a vibration is shown in Table 1. The measurement data were obtained at 40% and 70% relative density, which represented the sample conditions with the highest and lowest potential density of soil liquefaction. The measurement data was analyzed and compared to the liquefaction initiation value, ru, to indicate if liquefaction had occurred or not. Soil liquefaction occurs when the ru value equals or exceeds 1 (ru>1) [17].

Table 2. Excess pore water pressure measurement data at 1 Hz with 70% relative density

Time	Measurement results of excess pore water pressure (mbar)					
(second)	PT 1	PT 2	PT 3	ru 1	ru 2	ru 3
1	7.51	20.8	32.53	0.103991359	0.035884267	0.021255928
2	9.44	23.64	36.38	0.138257673	0.183688934	0.14764253
3	10.74	23.635	37.87	0.301430597	0.183428714	0.196555787
4	11.705	23.63	38.77	0.422555114	0.183168495	0.226100707
5	12.67	23.53	39.58	0.54367963	0.177964105	0.252691134
*	*	*	*	*	*	*
*	*	*	*	*	*	*
*	*	*	*	*	*	*
58	11.75	23.46	23.46	0.756634341	0.310418434	0.269489119
59	11.61	23.39	23.39	0.738619238	0.306683596	0.268142935
60	10.96	22.73	22.73	0.654977687	0.271469404	0.270835303

Table 3. Excess pore water pressure measurement data at 1.2 Hz with 40% relative density

Time	Measurement results of excess pore water pressure (mbar)					
(second)	PT 1	PT 2	PT 3	ru 1	ru 2	ru 3
1	5.87	20.14	33.30	0.020781709	0.005895709	0.047705379
2	14.53	21.81	42.68	1.114362822	0.089102576	0.363385421
3	15.81	27.93	46.53	1.279072339	0.41563417	0.492955588
4	15.83	27.94	46.92	1.281645925	0.415900945	0.506080878
5	15.72	27.94	47.65	1.267491201	0.416034332	0.530648727
*	*	*	*	*	*	*
*	*	*	*	*	*	*
*	*	*	*	*	*	*
58	8.72	20.82	35.06	0.047884977	0.036925145	0.104309981
59	9.02	20.89	34.99	0.085540267	0.040568218	0.102012043
60	9.04	21.18	35.06	0.08805062	0.055660948	0.104309981

Time : Data result in every second
PT 1 : Results of pore water pressure measurement on pressure transmitter 1
PT 2 : Results of pore water pressure measurement on pressure transmitter 2

PT 3	:	Results of pore water pressure measurement on pressure transmitter 3
ru 1	:	Initiation of soil liquefaction on pressure transmitter 1
ru 2	:	Initiation of soil liquefaction on pressure transmitter 2
ru 3	:	Initiation of soil liquefaction on pressure transmitter 3

Based on Table 2 and Table 3, the excess pore water pressure measurement system can measure the value of the change in pore water pressure in millibars (mbar) and observe the behaviour of the soil when liquefaction events occur and do not occur with an accuracy of 90.67% for pressure transmitter 1, 98.04% for pressure transmitter 2 and 98.38% for pressure transmitter 3, or an average accuracy of 95.69%. The saturated sand soil condition (addition of water to the soil sample) has a smooth surface.

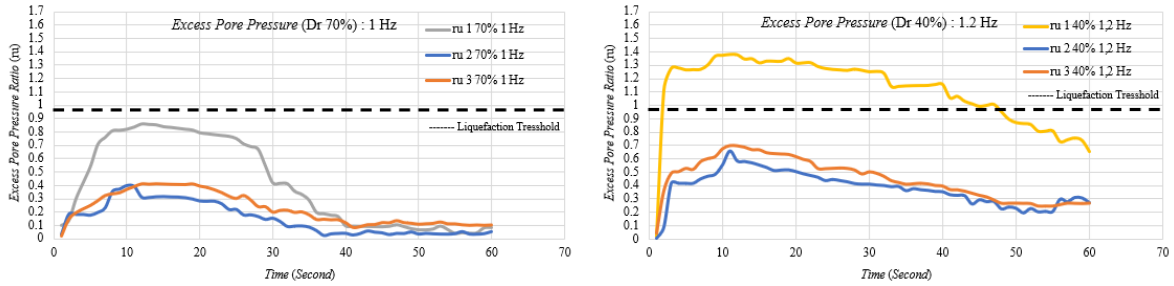

(a) (b)

Fig 8. (a) Excess pore water pressure (ru) at 1 Hz with a relative density of 70% (b) Excess pore water pressure (ru) at 1.2 Hz with a relative density of 40%.

As shown by Fig. 8, the ru values of each pressure transmitter indicate if liquefaction is occurring or not. Fig. 8(a) shows that soil liquefaction did not occur at pressure transmitter 1, with a relative density of 70% at 1 Hz, as the ru value was < 1. While Fig. 8(b) shows that at pressure transmitter 1 with a relative density of 40% at 1.2 Hz, soil liquefaction occurs because the value of ru > 1. So, it implied that this research can measure excess pore water pressure with different relative densities to determine soil behaviour when soil liquefaction occurs.

3.3 Response of displacement measurement

The displacement measurement data response was measured by the draw-wire sensor for 60 seconds or condition when vibration was given to the shaking table, as shown in Table 4. Table 4 shows that the measurement system can measure displacement in millimetres (mm), which is indicated by the measured value following the mechanical calculation or reference value, which is 50 mm. The measurement data was processed and the accuracy rate of the displacement measurement was 99.03%.

Note for Table 4:

Max	:	Result maximum value
Min	:	Result minimum value
Actual measurement data	:	Draw-wire sensor results in measurement of the amount of displacement on the plant table
Reference	:	Initiation of plant displacement
Time	:	Data result every second

Table 4. Displacement measurement data (mm)

Time (second)	Displacement measurement results (mm)				
	Max value of draw wire (mm)	Min value of draw wire (mm)	Actual measurement data (mm)	References (mm)	Error (%)
1	32.16	-20.18	52.34	50	
2	29.35	-20.87	50.22	50	
3	32.21	-20.98	53.19	50	
4	32.06	-18.73	50.79	50	
5	32.01	-20.92	52.93	50	
*	*	*	*	*	99.03
*	*	*	*	*	
*	*	*	*	*	
55	26.29	-21.18	47.47	50	
56	31.8	-21.08	52.88	50	
57	28.16	-21.44	6.72	50	

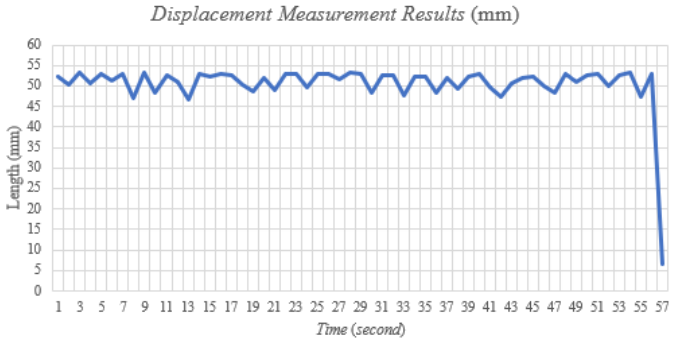

Fig 9. Displacement measurement data (mm)

Fig. 9 depicts the displacement value on the shaking table, which represents the state of the plant, changes when the plant is moved with an initial point of 50 mm and the plant moves 2.5 mm to the right or left.

3.4 Response of vibration acceleration and frequency measurement

Objective data on acceleration measurements and vibration frequency, were measured by the accelerometer for 60 seconds or when a vibration was given to the shaking table, as shown in Table 5 and Table 6. The acceleration value obtained in the measurement was processed using the FFT method to transform the signal from the time domain to the frequency domain.

Table 5. Accelerometer measurement data at 1 Hz

Time (second)	Measurement results of accelerometer sensor					
	ACC 1 (mg)	Freq 1 (Hz)	ACC 2 (mg)	Freq 2 (Hz)	Frequency reference (Hz)	Acceleration theory (mg)
1	7.51	20.8	32.53	0.103991359	0.035884267	0.021255928
2	9.44	23.64	36.38	0.138257673	0.183688934	0.14764253
3	10.74	23.635	37.87	0.301430597	0.183428714	0.196555787
4	11.705	23.63	38.77	0.422555114	0.183168495	0.226100707
5	12.67	23.53	39.58	0.54367963	0.177964105	0.252691134
*	*	*	*	*	*	*
*	*	*	*	*	*	*
*	*	*	*	*	*	*
58	11.75	23.46	23.46	0.756634341	0.310418434	0.269489119
59	11.61	23.39	23.39	0.738619238	0.306683596	0.268142935
60	10.96	22.73	22.73	0.654977687	0.271469404	0.270835303

Table 6. Accelerometer measurement data at 1.2 Hz

Time (second)	Measurement results of accelerometer sensor					
	ACC 1 (mg)	Freq 1 (Hz)	ACC 2 (mg)	Freq 2 (Hz)	Frequency reference (Hz)	Acceleration theory (mg)
1	78.53	3.02	87.29	2.2	1	100.51
2	78.53	3.02	87.29	2.2	1	100.51
3	78.53	3.02	87.29	2.2	1	100.51
4	77.405	3.105	91.46	1.66	1	100.51
5	76.28	3.19	95.63	1.12	1	100.51
*	*	*	*	*	*	*
*	*	*	*	*	*	*
*	*	*	*	*	*	*
43	73.91	1.27	142.18	0.64	1	100.51
44	73.91	1.27	142.18	0.64	1	100.51
45	73.91	1.27	142.18	0.64	1	100.51

Table 5 and Table 6 show the acceleration sensor measurements do not match the theoretical calculations due to the condition of the sensor, which was not calibrated regularly and the validation process was not carried out due to the lack of other measuring instruments to compare the sensor readings with other parameters, so the accuracy level of the sensor became low, as shown in Table 7.

Table 7. Calculation of error of accelerometer measurement

Subject (%)	Calculation of error of accelerometer measurement at 1 Hz VFD condition.					
	ACC 1 (mg)	Freq 1 (Hz)	ACC 2 (mg)	Freq 2 (Hz)	Frequency reference (Hz)	Acceleration theory (mg)
Error	36.47%	57.03%	55.93%	40.04%	0.80	64.32
Accuracy	63.53%	42.97%	44.07%	59.96%		

Subject (%)	Calculation of error of accelerometer measurement at 1.2 Hz VFD condition.					
	ACC 1 (mg)	Freq 1 (Hz)	ACC 2 (mg)	Freq 2 (Hz)	Frequency reference (Hz)	Acceleration theory (mg)
Error	29.73%	78.22%	11.94%	4.36%	0.80	64.32
Accuracy	70.27%	21.78%	88.06%	95.64%		

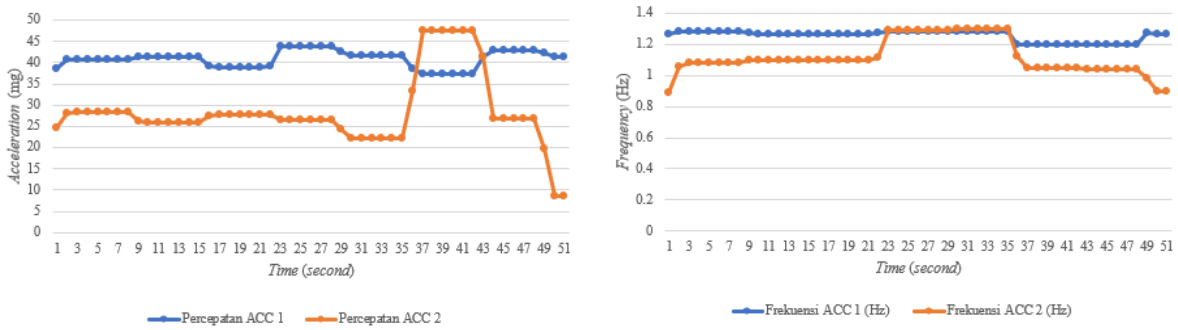

Fig 10. Accelerometer measurement at 1 Hz

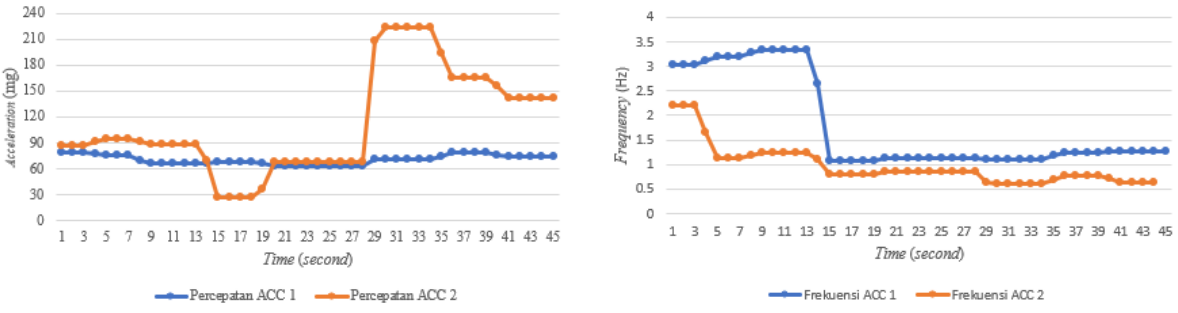

Fig 11. Accelerometer measurement at 1.2 Hz

As shown in Fig. 10 and Fig. 11, the acceleration and vibration frequency value change is not good enough because the measurement results cannot approach the reference value due to the mismatch between the sensor output and the datasheet.

4. Conclusion

Based on the research and discussion results, it can be concluded that the frequency adjustment system to adjust the motor speed, as well as the measurement system of pore pressure response on the ground, acceleration, and vibration frequency, can be used to do adjustment and measurement integrated with LabVIEW software. The motor speed is directly proportional to the input frequency in the created frequency regulation system. In addition, the frequency received by the motor is also influenced by the presence and absence of loads, as shown by the error value of 1.65% when no load is added, while the error value is 8.71% when a load is added. Then, the measurement of excess pore water pressure is able to measure changes in pore water pressure so that the behaviour of the soil when liquefaction events occur or do not occur can be observed with an average level of accuracy of the three pressure transmitters of 95.69%. Meanwhile, the displacement measurement system implemented is able to measure the displacement or displacement of the shaking table deviation with a sensor accuracy level of 99.03%. The implemented acceleration and vibration frequency measurement system revealed that the accelerometer sensors used did not qualify as measuring instruments with a low sensor accuracy level of 67.9% for accelerometer 1 and 66.06% for accelerometer 2.

Acknowledgement

The authors would like to thank Jakarta State Polytechnic for supporting this research through the Final Year Student Research Programme, and the Department of Electrical Engineering and Civil Engineering, Jakarta State Polytechnic for facilitating the development of the system.

References

[1] X. Ding, Y. Zhang, Q. Wu, Z. Chen, and C. Wang, "Shaking table tests on the seismic responses of underground structures in coral sand," *Tunnelling and Underground Space Technology*, vol. 109, Mar. 2021, doi: 10.1016/j.tust.2020.103775.

[2] Y. Cao, Z. Qu, and X. Ji, "A novel control strategy for reproducing the floor motions of high-rise buildings by earthquake-simulating shake tables," *Earthquake Research Advances*, p. 100236, May 2023, doi: 10.1016/j.eqrea.2023.100236.

[3] X. Feng, B. Ye, J. He, H. Miao, and C. Lin, "Shaking table test on underwater slope failure induced by liquefaction," *Soils and Foundations*, vol. 63, no. 4, Aug. 2023, doi: 10.1016/j.sandf.2023.101357.

[4] A. Bahmanpour, I. Towhata, M. Sakr, M. Mahmoud, Y. Yamamoto, and S. Yamada, "The effect of underground columns on the mitigation of liquefaction in shaking table model experiments," *Soil Dynamics and Earthquake Engineering*, vol. 116, pp. 15–30, 2019, doi: https://doi.org/10.1016/j.soildyn.2018.09.022.

[5] F. Ou Yang, G. Fan, K. Wang, C. Yang, W. Lyu, and J. Zhang, "A large-scale shaking table model test for acceleration and deformation response of geosynthetic encased stone column composite ground," *Geotextiles and Geomembranes*, vol. 49, no. 5, pp. 1407–1418, 2021, doi: https://doi.org/10.1016/j.geotexmem.2021.05.013.

[6] F. Xu *et al.*, "Shaking table test on seismic response of a planar irregular structure with differential settlements of foundation," *Structures*, vol. 46, pp. 988–999, 2022, doi: https://doi.org/10.1016/j.istruc.2022.10.090.

[7] F. Ou Yang, G. Fan, K. Wang, C. Yang, W. Lyu, and J. Zhang, "A large-scale shaking table model test for acceleration and deformation response of geosynthetic encased stone column composite ground," *Geotextiles and Geomembranes*, vol. 49, no. 5, pp. 1407–1418, Oct. 2021, doi: 10.1016/j.geotexmem.2021.05.013.

[8] R. Motamed, V. Sesov, I. Towhata, and N. T. Anh, "Experimental Modeling of Large Pile Groups in Sloping Ground Subjected to Liquefaction-Induced Lateral Flow: 1-G Shaking Table Tests," *Soils and Foundations*, vol. 50, no. 2, pp. 261–279, 2010, doi: https://doi.org/10.3208/sandf.50.261.

[9] X. Feng, B. Ye, J. He, H. Miao, and C. Lin, "Shaking table test on underwater slope failure induced by liquefaction," *Soils and Foundations*, vol. 63, no. 4, Aug. 2023, doi: 10.1016/j.sandf.2023.101357.

[10] S. Kockanat, "Acceleration harmonics estimation and elimination with MABC–RLS algorithm: Simulation and experimental analyses on shaking table," *Applied Soft Computing Journal*, vol. 92, Jul. 2020, doi: 10.1016/j.asoc.2020.106377.

[11] A. Ghalandarzadeh, S. Rahimi, and A. Kavand, "Dynamic pore water pressure of submerged backfill on caisson quay walls: 1 g shake table tests," *Soil Dynamics and Earthquake Engineering*, vol. 132, p. 106091, 2020, doi: https://doi.org/10.1016/j.soildyn.2020.106091.

[12] X. Zhang, A. R. Russell, and X. Dong, "Liquefaction responses of fibre reinforced sand in shaking table tests with a laminated shear stack," *Soil Dynamics and Earthquake Engineering*, vol. 162, p. 107466, 2022, doi: https://doi.org/10.1016/j.soildyn.2022.107466.

[13] S. Nokande, Y. Jafarian, and A. Haddad, "Shaking table tests on the liquefaction-induced uplift displacement of circular tunnel structure," *Underground Space*, vol. 10, pp. 182–198, 2023, doi: https://doi.org/10.1016/j.undsp.2022.09.004.

[14] Y.-Y. Ko, Y.-T. Li, C.-H. Chen, S.-Y. Yeh, and S.-Y. Hsu, "Influences of repeated liquefaction and pulse-like ground motion on the seismic response of liquefiable ground observed in shaking table tests," *Eng Geol*, vol. 291, p. 106234, 2021, doi: https://doi.org/10.1016/j.enggeo.2021.106234.

[15] S. Song and S. Jeong, "Dynamic analysis of a single Pile embedded in SM soil using 1-g shaking table tests," *Ocean Engineering*, vol. 285, p. 115416, 2023, doi: https://doi.org/10.1016/j.oceaneng.2023.115416.

[16] S. Islami, O. Candra, Aswardi, and R. Maulana, "Modul 3 Instalasi Tenaga Listrik" 2019.

[17] H. Hazarika *et al.*, "Strain Criterion for Initiation of Liquefaction Using Shake Table Test," *International Journal of Geotechnical Engineering*, vol. 30, no. 5, pp. 162–174, 2018.